

Article

First-Principles Study for Gas Sensing of Defective SnSe₂ Monolayers

Wei-Ying Cheng ¹, Huei-Ru Fuh ² and Ching-Ray Chang ^{3,*}

¹ Graduate Institute of Applied Physics, National Taiwan University, Taipei 10617, Taiwan; weiyiing@phys.ntu.edu.tw

² Department of Chemical Engineering & Materials Science, Yuan Ze University, Taoyuan 32003, Taiwan; hrfuh@saturn.yzu.edu.tw

³ Department of Physics, National Taiwan University, Taipei 10617, Taiwan

* Correspondence: crchang@phys.ntu.edu.tw; Tel.: +886-2-3366-5176

Received: 10 January 2020; Accepted: 24 February 2020; Published: 29 February 2020



Abstract: We report the interaction between gas molecules (NO₂ and NH₃) and the SnSe₂ monolayers with vacancy and dopants (O and N) for potential applications as gas sensors. Compared with the gas molecular adsorbed on pristine SnSe₂ monolayer, the Se-vacancy SnSe₂ monolayer obviously enhances sensitivity to NO₂ adsorption. The O-doped SnSe₂ monolayer shows similar sensitivity to the pristine SnSe₂ monolayer when adsorbing NO₂ molecule. However, only the N-doped SnSe₂ monolayer represents a visible enhancement for NO₂ and NH₃ adsorption. This work reveals that the selectivity and sensitivity of SnSe₂-based gas sensors could be improved by introducing the vacancy or dopants.

Keywords: SnSe₂; defect; O-doped; N-doped; gas sensors; first-principle study

1. Introduction

Recently, two-dimensional transition metal dichalcogenide (2D-TMD) materials have gained great attention due to their unique structural and electrical properties. Since graphene was introduced into the research, other families of 2D materials with layered structures are also fast emerging for some better applications. 2D-TMD materials with a narrow tunable band gap and replaceable cation and anion [1–3] are more advantageous than the pristine graphene which lacks band gap. SnSe₂, a IV–VI semiconductor, has been widely studied for optoelectronic and thermoelectric applications [4,5]. For example, SnSe₂ is used as a high-performance photodetector that shows relatively fast photoresponse at room temperature with a high photo-to-dark ratio [4].

2D-TMDs materials have been applied as gas sensors due to their large surface-area-to-bulk ratio. The layered SnX₂ (X = S, Se) nanosheets show a significant sensitivity to individual molecules, such as NO₂ and NH₃ [3,6–8]. The SnX₂ (X = S, Se)-based gas sensors show a good response to NO₂ at room temperature [6–8]. Furthermore, the SnSe₂ monolayer shows a higher sensitivity for NO₂ molecule adsorption than SnS₂ in our related work [7,8]. Also, the charge transfers and the flat band contributed by gas adsorption induces the conductivity difference of the SnSe₂ monolayer reported in our previous study [8].

More recently, the doped SnSe₂ nanosheets have been widely studied because of its interesting electronic and optoelectronic properties, [9–13]. Huang et al. [9] systematically studied n-type/p-type and isoelectronic doping cases on SnSe₂ nanosheets based on density functional theory (DFT). Huang et al. [9] suggest that P and As are not promising candidates for p-type doping because those atoms contribute trap states near the Fermi level (E_F). Although the N atom is a promising candidate for p-type doping which induces states near the valence band maximum (VBM), it is difficult to achieve

the N-doped SnSe₂ in reality. For O-, S-, Te-doped SnSe₂, the density of states (DOS) of all doped SnSe₂ are similar to that of pristine SnSe₂ monolayer [9]. On the other hand, n-type doping of F, Cl and Br are highly recommended, especially Br, since the states near both the VBM and the conduction band minimum (CBM) result in a high carrier density and conductivity [10–12]. For the gas sensor, the SnSe₂ monolayer demonstrates a high sensitivity and charge transfer to NO₂ [8].

The defective graphene would enhance sensitivity for gas sensing which has been theoretically and experimentally reported [14,15]. Zhang et al. [14] theoretically reveal that the defective graphene has stronger interaction with CO, NO and NO₂ than the pristine graphene. Also, the B-doped graphene gives the tightest binding with NH₃. Lee et al. [15] demonstrate the defect-engineered graphene oxide chemical sensors, which exhibit ultrahigh sensitivity for NO₂ and NH₃ from the experimental data. However, there is no related study regarding the gas-sensing properties of the doped SnSe₂ nanosheets.

In this work, on the basis of DFT, we investigate the gas detection properties for NO₂ and NH₃ adsorbed on the defective SnSe₂ monolayer by substitution of the Se site with a single vacancy, O or N atoms. To the best of our knowledge, the gas sensors of the defective SnSe₂ monolayers are investigated for the first time. In order to understand the sensing mechanism, we report adsorption energy, charge transfer, DOS and structural parameters of gas molecules adsorption on defective SnSe₂ monolayers. We also discuss and compare the gas-sensing parameters of defective SnSe₂ monolayers with the pristine SnSe₂ monolayer. We find that the vacancy and doped SnSe₂ monolayer can enhance the selectivity and sensitivity of gas sensing.

2. Method

The SnSe₂ monolayer structure is based on the experimental lattice parameters of bulk SnSe₂ [16]. The initial lattice constants of SnSe₂ monolayer are $a = b = 3.81 \text{ \AA}$ and thickness of vacuum is set about 16 Å. All calculated structures contain the fully lattice constants and atom positions optimization. After structure optimization, the lattice constants of the SnSe₂ monolayer are $a = b = 3.87 \text{ \AA}$ and the energy gap is 0.78 eV. The Visualization for Electronic and Structural Analysis (VESTA) software is a 3D visualization program for structural models [17]. We use VESTA to show the crystal structure and the defective single layer in this work. The calculation was implemented in the Vienna Ab initio Simulation Package (VASP) and performed by the projector augmented wave (PAW) method with the Perdew–Burke–Ernzerhofer (PBE) generalized gradient approximation (GGA) [18,19]. The SnSe₂ monolayer is constructed with a $3 \times 3 \times 1$ supercell in order to perform gas molecules adsorption calculation. The energy cutoff for a plane-wave basis was set up to 400 eV within the $12 \times 12 \times 1$ Monkhorst–Pack k -point grid for all study cases. The energy convergence threshold and force convergence criteria were set to 10^{-5} eV per unit cell and 0.01 eV \AA^{-1} .

We also discussed the vacancy and doped SnSe₂ monolayers that adsorb NO₂ and NH₃ gas molecules. First of all, we put the NO₂ and NH₃ molecules on 3 Å above the Se site or the dopants. We calculated two orientations of N atom, the N atom of gas molecules toward and backward the defective SnSe₂ monolayers, named N-bottom and N-top, respectively. In order to understand the defect effect of SnSe₂ monolayers adsorbing gas molecule, a Se atom was substituted by a vacancy or a dopant atom (N and O). In this paper, the structures of the SnSe₂ monolayers with gas adsorption were relaxed. The initial configurations for gases adsorption on the defective SnSe₂ monolayers are illustrated in Figures S1 and S2 of the supplementary material.

3. Results

3.1. SnSe₂ Monolayers

The pristine 1T phase SnSe₂ monolayer is a hexagonal crystal structure as shown in Figure 1a. A Sn atom is sandwiched between two Se atoms which form a Se–Sn–Se arrangement with ABC stacking as shown in Figure 1e. The defective SnSe₂ monolayer with Se vacancy in the center of supercell is represented in Figure 1b,f. Figure 1c,g are the defective SnSe₂ monolayer in which a Se

atom is substituted by O atom. Furthermore, Figure 1d,h are the defective SnSe₂ monolayer in which a Se atom is substituted by a N atom. The O and N dopants are sucked into the vacancy site as shown in Figure 1g,h.

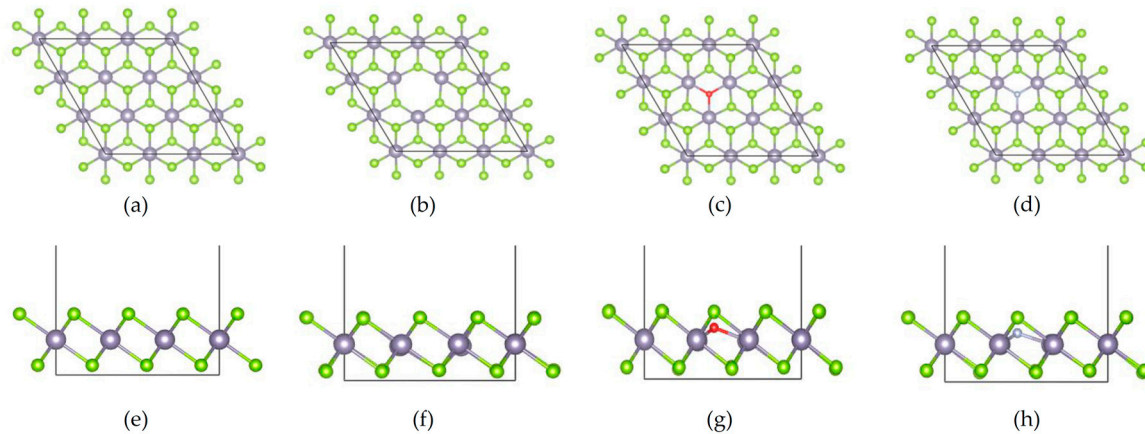


Figure 1. The structures of different SnSe₂ monolayer systems which including the top view of (a) pristine, (b) Se vacancy, (c) O-doped and (d) N-doped SnSe₂ monolayer and the side view of (e) pristine, (f) Se vacancy, (g) O-doped and (h) N-doped SnSe₂ monolayer, respectively. The Sn, Se, O, and N atom are purple, green, red and grey, respectively.

Figure 2 is the DOS with or without defects on the SnSe₂ monolayer. The pristine SnSe₂ monolayer has an indirect band gap of 0.78 eV as shown in Figure 2a, which is consistent with the previous reported value [8,20]. In the Se-vacancy SnSe₂ monolayer, there are occupied states very near E_F as shown in Figure 2b. However, the DOS are very different between the O-doped and the N-doped SnSe₂ monolayer. The DOS of the O-doped SnSe₂ monolayer is similar to the pristine SnSe₂ monolayer with the energy gap 0.84 eV because the states contributed from impurities are far from E_F , as shown in Figure 2c. The resultant impurity state from the doped O atom is near the band edge, above 0.8 eV and below -0.1 eV denoted by the orange line in Figure 2c. For the N-doped SnSe₂ monolayer, the partial density of state (PDOS) induced by the N dopant is near VBM denoted by the blue line in Figure 2d. The DOS of the SnSe₂ monolayer with N and O dopant also is consistent with the result of Huang et al. [9].

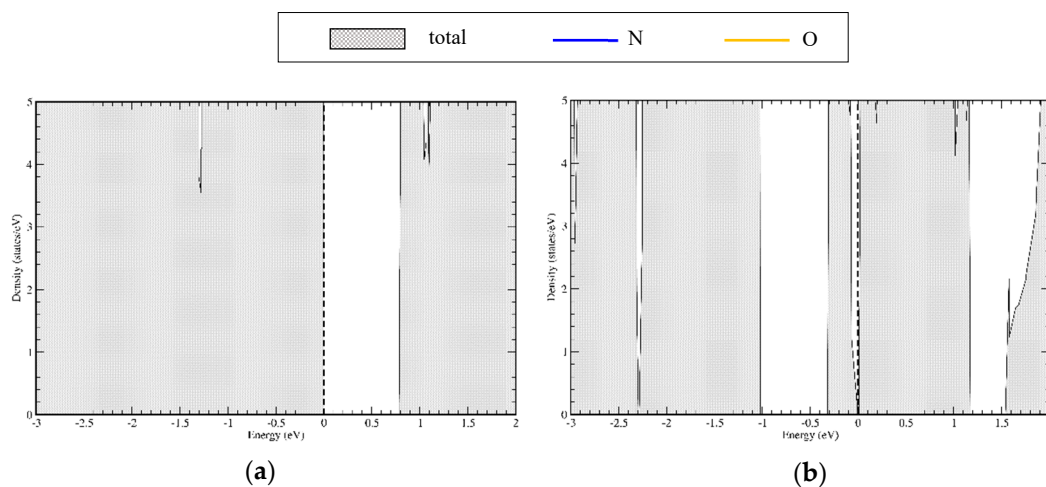


Figure 2. Cont.

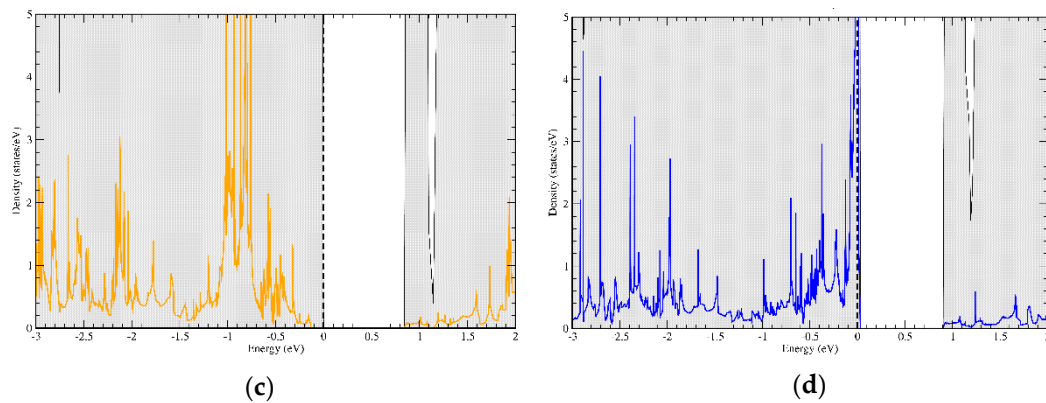


Figure 2. The density of states (DOS) of the (a) pristine, (b) Se vacancy, (c) O-doped and (d) N-doped SnSe₂ monolayer. The shadowed area is the total DOS. The blue and orange lines are the partial density of state (PDOS) of N and O atoms, respectively. The E_F is denoted by a dashed line and shift to zero.

3.2. Gases Adsorbed on Different SnSe₂ Monolayers

In this section, we discuss the most stable configurations of NO₂ and NH₃ molecules adsorbed on different SnSe₂ monolayer systems, which are listed in Table 1.

Table 1. The most stable structural configurations of different gas molecules adsorbed on SnSe₂ monolayer systems. E_{ad}, d_{atom-atom}, h and ΔQ_b of molecules adsorbed on the pristine and defective SnSe₂ monolayers.

Gas	SnSe ₂ System	Gas Orientation	E _{ad} (eV)	d _{atom-atom} (Å)	h (Å)	ΔQ _b	Source
NO ₂	Pristine	N-top	−0.29	2.97	2.45	−0.164e	Reference [8]
	Se vacancy	N-bottom	−1.84	2.28	−0.08	−0.926e	This work
	O-doped	N-top	−0.32	3.05	1.75	−0.145e	This work
	N-doped	N-bottom	−2.98	1.38	0.72	−0.368e	This work
NH ₃	Pristine	N-bottom	−0.18	3.35	2.47	0.028e	Reference [8]
	Se vacancy	N-bottom	−0.82	2.90	0.45	0.016e	This work
	O-doped	N-top	−0.13	3.06	1.93	0.000e	This work
	N-doped	N-bottom	−0.36	2.46	1.45	0.215e	This work

The adsorption energy (E_{ad}) of gas molecules on SnSe₂ monolayers is defined as

$$E_{ad} = E_{Gas + SnSe_2} - E_{SnSe_2} - E_{Gas}, \quad (1)$$

where E_{Gas + SnSe₂} is the total energy of the gas molecules adsorbed on SnSe₂ monolayers, E_{SnSe₂} is the total energy of the SnSe₂ monolayer and E_{Gas} is the energy of isolated gas molecule. A negative E_{ad} value means that gas molecules on the SnSe₂ monolayer is energetically favorable. In our previous work [8], the adsorption energy of NO₂ adsorbed on the pristine SnSe₂ monolayer is higher than that of NH₃ adsorption in theoretical prediction. In experimental demonstrations, the pristine SnSe₂ monolayer can detect NO₂ in lower concentrations than NH₃. Although the value of adsorption energy is not direct and not the only relation to the sensitivity, both of them could coincide in terms of theoretical calculation and experimental measurements. Generally, the E_{ad} values of NO₂ on SnSe₂ monolayer systems (−0.29 to −2.98 eV) are larger than NH₃ (−0.13 to −0.82 eV). This indicates that the sensitivity of NO₂ is higher than NH₃ on SnSe₂ monolayers. Moreover, the distance between NO₂ and SnSe₂ monolayers is smaller than the distance between NH₃ and SnSe₂ monolayer.

The Bader charge population analysis [21] is summarized in Table 1 where negative ΔQ_b indicates electron charge transfer from SnSe₂ to a gas molecule and a positive ΔQ_b shows charge transfer from a gas molecule to SnSe₂ monolayers. Our calculation shows that the NO₂ is an electron charge acceptor,

whereas NH_3 is an electron charge donor in all of the study cases. Moreover, the absolute values of ΔQ_b for NO_2 adsorbed on SnSe_2 monolayers are greater than that for NH_3 adsorbed on SnSe_2 monolayers.

In Table 1, we use the two parameters, $d_{\text{atom-atom}}$ and h , to describe the position of gas molecules adsorbed on the SnSe_2 monolayers. The $d_{\text{atom-atom}}$ means the shortest distance between the lowest atom of a gas molecule and the highest atom of SnSe_2 monolayer. The h indicates the vertical distance between them. We mark $d_{\text{atom-atom}}$ and h in the structure of gas adsorbed on the SnSe_2 monolayers to compare the positions of gas adsorption in different SnSe_2 monolayers. This would be shown in following figures. Furthermore, we also discuss the h , E_{ad} and ΔQ_b to analyze the gas-sensing mechanism for defective SnSe_2 monolayers as shown in Table 1.

In the following sections, the detail will be discussed about adsorption energy, charge transfer, DOS and structural parameters of gas molecules adsorption on defective SnSe_2 monolayers.

3.2.1. NO_2 Adsorption

Figure 3 shows the optimized structures of NO_2 adsorbed on SnSe_2 monolayers, including top views as shown in Figure 3a–d and side views, as shown in Figure 3e–h. When NO_2 is adsorbed on the pristine SnSe_2 monolayer, the site of NO_2 adsorption is near the Se atom, the $d_{\text{O-Se}}$ is 2.97 Å and the orientation is N-top, as shown in Figure 3a,e. When NO_2 is adsorbed on the Se-vacancy SnSe_2 monolayer, the site is near the Sn atom, the $d_{\text{O-Sn}}$ is 2.28 Å and the orientation is N-bottom, as shown in Figure 3b,f. The optimized structure of NO_2 on the O-doped SnSe_2 monolayer is upon the site of the O atom, the $d_{\text{O-O}}$ is 3.05 Å and the orientation is N-top, as shown in Figure 3c,g. The optimized structure of NO_2 on the N-doped SnSe_2 monolayer is located on the N site and the $d_{\text{N-N}}$ is 1.38 Å with the orientation N-bottom, as shown in Figure 3d,h. Moreover, the vertical distances h between NO_2 and the defective SnSe_2 monolayers are 2.45 Å, -0.08 Å, 1.75 Å, 0.72 Å, respectively. The negative value of h means the gas molecule is sucked into the SnSe_2 monolayer. In conclusion, the values of h between NO_2 and the defective SnSe_2 monolayer are shorter than NO_2 adsorbed on the pristine SnSe_2 monolayer. When comparing with orientation and the h , the structures of NO_2 adsorbed on the SnSe_2 monolayers could divide into two groups. First, the NO_2 adsorption on the pristine and O-doped SnSe_2 monolayer are both N-top orientation. Second, the NO_2 adsorption on the Se-vacancy and N-doped SnSe_2 monolayer are both with N-bottom orientation. The values of h are smaller for NO_2 adsorption on the Se-vacancy and N-doped SnSe_2 monolayer than those on the pristine and O-doped SnSe_2 monolayer.

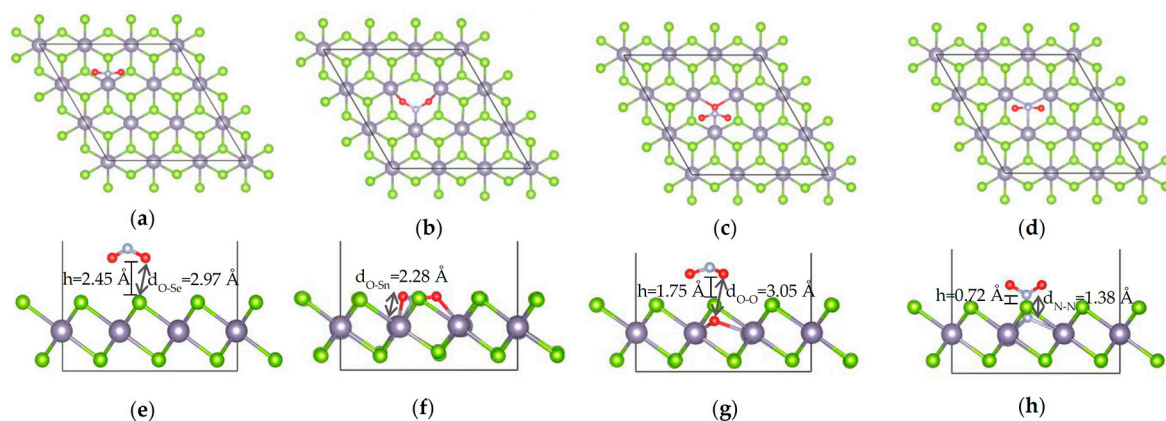


Figure 3. The most stable configurations of different SnSe_2 monolayers adsorbing NO_2 molecule. The top view of (a) pristine, (b) Se vacancy, (c) O-doped and (d) N-doped SnSe_2 monolayer; the side view of (e) pristine, (f) Se vacancy, (g) O-doped and (h) N-doped SnSe_2 monolayer, respectively. The Sn, Se, O, and N atom are purple, green, red and grey, respectively.

The value of E_{ad} and ΔQ_b of NO_2 adsorbed on the pristine SnSe_2 monolayer are -0.29 eV and $-0.164e$, respectively [8]. Furthermore, the E_{ad} of NO_2 adsorbed on the Se-vacancy and doped SnSe_2 monolayer are greater than NO_2 adsorbed on the pristine SnSe_2 monolayer, as shown in Table 1.

The value of h between NO_2 and the Se-vacancy SnSe_2 monolayer is -0.08 Å. This induces a large adsorption energy and Bader charge because the NO_2 molecule is sucked into the vacancy site. The E_{ad} and ΔQ_b are up to -1.84 eV and $-0.926e$, respectively, as listed in Table 1. The value of E_{ad} is greater than the pristine and the O-doped SnSe_2 monolayer but smaller than the N-doped SnSe_2 system. The value of $\Delta Q_b = -0.926e$ of NO_2 adsorbed on the Se-vacancy SnSe_2 monolayer is the maximum of that on the SnSe_2 monolayers. This result indicates that NO_2 molecule would strongly interact with the Se-vacancy SnSe_2 monolayer.

As mentioned, the structure of NO_2 adsorbed on the O-doped SnSe_2 monolayer is similar with on the pristine SnSe_2 monolayer despite of the O atom replacing the Se atom. In the detail, the value of h between NO_2 and the O-doped SnSe_2 monolayer is 1.75 Å, which is also a little smaller than that on the pristine SnSe_2 monolayer. Furthermore, the O-doped SnSe_2 monolayer adsorbs the NO_2 molecule and would induce a little increase in the adsorption energy but decrease the Bader charge by about -0.32 eV and $-0.145e$, respectively, as shown in Table 1.

When NO_2 is adsorbed on the N-doped SnSe_2 monolayer, the value of h between NO_2 and the N-doped SnSe_2 monolayer is 0.72 Å. This indicates that the strong interaction comes from the N-N atoms interaction between NO_2 and the N dopant. The $E_{ad} = -2.98$ eV of NO_2 adsorbed on the N-doped SnSe_2 monolayer is greater than on the Se-vacancy SnSe_2 monolayer. $\Delta Q_b = -0.368e$ of NO_2 adsorbed on the N-doped SnSe_2 monolayer is smaller than on the Se-vacancy SnSe_2 , but greater than the pristine and O-doped SnSe_2 . The relatively high E_{ad} and ΔQ_b demonstrate strong interaction between NO_2 and the N-doped SnSe_2 monolayer.

The DOS of NO_2 adsorbed on different SnSe_2 monolayers is shown in Figure 4. The shadowed area is the total DOS. The blue and orange lines are the PDOS of N and O, respectively. The E_F is denoted by a dashed line. DOS of NO_2 adsorption on different SnSe_2 monolayers, as shown in Figure 4a–d, are quite different to Figure 2a–d without NO_2 adsorption cases. This indicates that all the SnSe_2 monolayers could induce obvious difference of electronic structure before/after NO_2 adsorption.

When NO_2 is adsorbed on the pristine SnSe_2 , the total DOS presents a trap state across E_F in the energy range about -0.04 eV to -0.02 eV, as shown in Figure 4a. A large amount of PDOS induced by N and O atoms of gas molecule is located in the aforementioned trap state, which induces the flat band and trap electron on it as mentioned in previous work [8]. The pattern of DOS in Figure 4a is different from DOS of the pristine SnSe_2 monolayer without adsorption as shown in Figure 2a.

For NO_2 adsorption on the Se-vacancy SnSe_2 monolayer, the total DOS presents a bandwidth near the E_F with an energy range of -0.19 eV to -0.12 eV, as shown in Figure 4b. A considerable amount of PDOS contributed by N and O atoms of the gas molecule is located the aforementioned bandwidth. Therefore, the pattern of DOS in Figure 4b is quite different from DOS of the Se-vacancy SnSe_2 without adsorption as shown in Figure 2b.

When NO_2 is adsorbed on the O-doped SnSe_2 monolayer, the total DOS presents a trap state across E_F in the energy range about -0.06 eV to -0.03 eV, as shown in Figure 4c. A large amount of PDOS induced by N and O atoms of the gas molecule is located in the aforementioned trap state, which corresponds to a flat band. The trap state would trap electrons on it and decrease the carrier mobility. The DOS of NO_2 adsorption the O-doped SnSe_2 monolayer is very similar with the pristine SnSe_2 monolayer, but different from the O-doped SnSe_2 monolayer without adsorption as shown in Figure 2c.

For NO_2 adsorption on the N-doped SnSe_2 monolayer, the total DOS shown in Figure 4d demonstrates a pattern for a semiconductor with an energy gap of about 0.86 eV. The PDOS introduced by N and O atoms of gas molecule below E_F and above 0.86 eV marked in blue and orange lines as shown in Figure 4d, which is quite different from Figure 4a–c. It is worth noting that the peak of PDOS of the N atom near the E_F shifts to -0.20 eV when NO_2 is adsorbed as shown in Figure 4d. It indicates

that PDOS of the N atoms near E_F in Figure 2d are moved to below E_F because the strong interaction occurred after NO_2 adsorption.

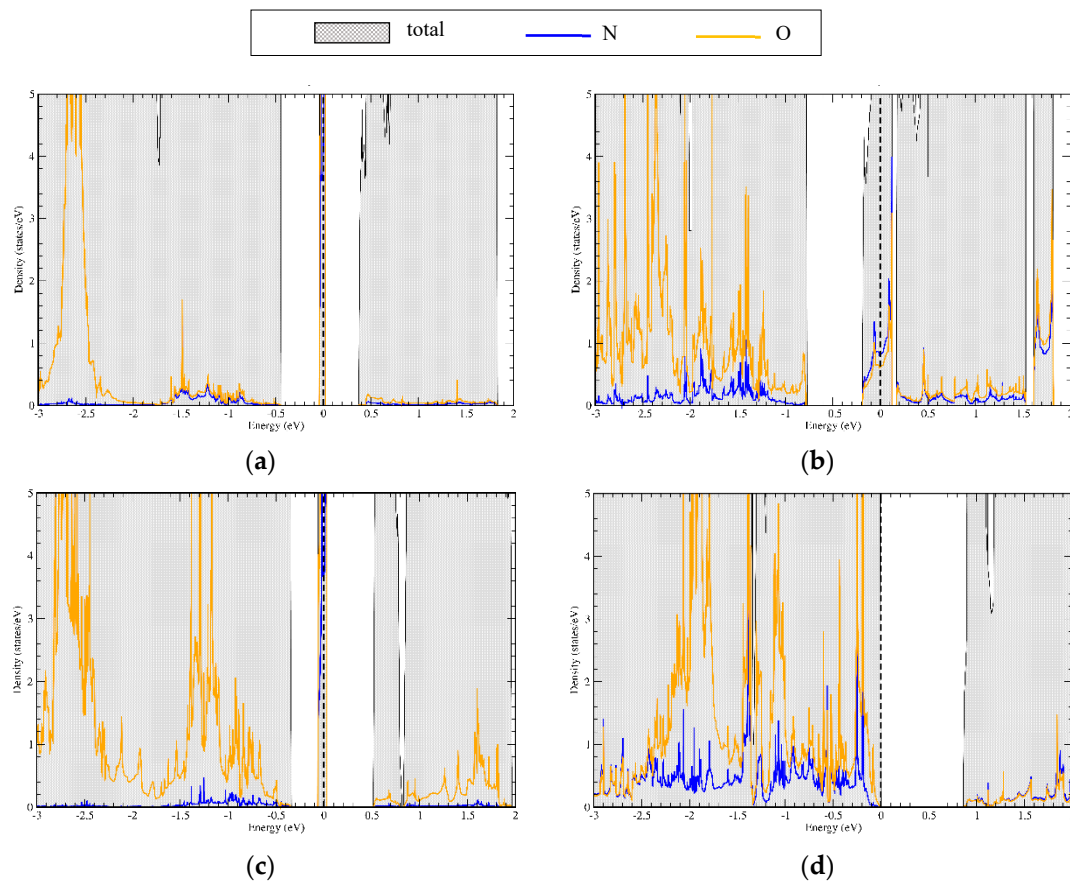


Figure 4. DOS of NO_2 adsorption on the (a) pristine, (b) Se-vacancy, (c) O-doped and (d) N-doped SnSe_2 monolayer. The shadowed area is the total DOS. The blue and orange lines are the PDOS of N and O, respectively. The E_F is denoted by a dashed line and shift to zero.

3.2.2. NH_3

Figure 5 shows the optimized structures of NH_3 adsorbed on SnSe_2 monolayers, including top views as shown in Figure 5a–d and side views as shown in Figure 5e–h. When NH_3 is adsorbed on the pristine SnSe_2 monolayer, the site is positioned above the Sn atom, the $d_{\text{N-Se}}$ is 3.35 Å and the orientation is N-bottom as shown in Figure 5a,e. When NH_3 is adsorbed on the Se-vacancy SnSe_2 monolayer, the site is positioned above the site of the single vacancy, the $d_{\text{H-Se}}$ is 2.90 Å and the orientation is N-bottom, as shown in the Figure 5b,f. The most stable configuration of NH_3 adsorbed on the O-doped SnSe_2 monolayer is positioned at the O site, the $d_{\text{H-O}}$ is 3.06 Å and the orientation is N-top as shown in Figure 5c,g. The optimized structure of NH_3 adsorbed on the N-doped SnSe_2 monolayer is positioned on the N site, the $d_{\text{N-N}}$ is 2.46 Å and the orientation is N-bottom as shown in Figure 5d,h. It is worth noting that the orientation of NH_3 adsorbed on O-doped SnSe_2 monolayer is different from the other SnSe_2 monolayers, which is N-top orientation but others are N-bottom. The vertical distances h between NH_3 and the different SnSe_2 monolayers are 2.47 Å, 0.45 Å, 1.93 Å, 1.45 Å as shown in Figure 5e–h, respectively. The values of h of NH_3 adsorbed on the Se-vacancy and doped SnSe_2 monolayer are smaller than NH_3 adsorbed on the pristine SnSe_2 monolayer.

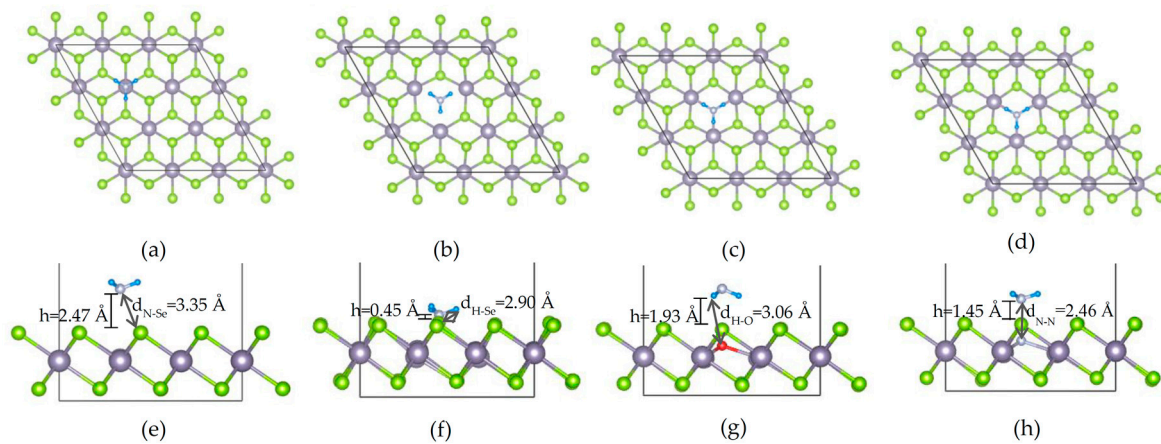


Figure 5. The most stable configurations of different SnSe₂ monolayers adsorbing NH₃ molecule. The top view of (a) pristine, (b) Se vacancy, (c) O-doped and (d) N-doped SnSe₂ monolayer; the side view of (e) pristine, (f) Se vacancy, (g) O-doped and (h) N-doped SnSe₂ monolayer, respectively. The Sn, Se, O, N and H atoms are purple, green, red, grey and cyan, respectively.

When NH₃ is adsorbed on the pristine SnSe₂ monolayer, the value of h , E_{ad} and ΔQ_b are 2.47 Å, −0.18 eV and 0.028e [8], respectively. Compared to the value of E_{ad} and h in the Table 1, the E_{ad} of NH₃ adsorption almost follows a positive correlation to h , except for NH₃ adsorption on the O-doped SnSe₂ monolayer.

When NH₃ is adsorbed on the Se-vacancy SnSe₂ monolayer, the value of $h = 0.45$ Å is the minimum among NH₃ adsorption on SnSe₂ monolayers. Furthermore, the value of $E_{ad} = -0.82$ eV of NH₃ on the Se-vacancy SnSe₂ monolayer reaches the maximum compared with other cases. However, the charge transfer amount $\Delta Q_b = 0.016e$ of NH₃ adsorbed on the Se-vacancy SnSe₂ monolayer is smaller than gas molecule on the pristine SnSe₂ (0.028e).

For NH₃ adsorption on the O-doped SnSe₂ monolayer, the value of $h = 1.93$ Å between NH₃ and the O-doped SnSe₂ monolayer is smaller than that on the pristine SnSe₂ monolayer. The values of E_{ad} and ΔQ_b of NH₃ on the O-doped SnSe₂ monolayer are −0.13 eV and 0.000e, which are both the minimum among the NH₃ adsorption. This indicates that the ability of NH₃ adsorption of the O-doped SnSe₂ monolayer is weaker than the pristine SnSe₂ monolayer.

For NH₃ adsorption on the N-doped SnSe₂ monolayer, the value of $h = 1.45$ Å between NH₃ and the O-doped SnSe₂ monolayer is smaller than that on the pristine SnSe₂ monolayer. E_{ad} also has a greater value −0.36 eV than that on the pristine SnSe₂ monolayer, and ΔQ_b of NH₃ on the N-doped SnSe₂ monolayer has a maximum value 0.215e. This shows an enhancement of NH₃ adsorption on the N-doped SnSe₂ monolayer.

Figure 6 shows DOS of NH₃ adsorption on different SnSe₂ monolayers. The blue, orange, cyan lines are the PDOS of N, O, H, respectively. The DOS of NH₃ adsorption on the pristine SnSe₂ monolayers demonstrates a pattern of a semiconductor with energy gap as shown in Figure 6a. However, the DOS of NH₃ adsorption on the defective SnSe₂ monolayers presents a flat band as shown in Figure 6b–d.

When NH₃ adsorbed on the pristine SnSe₂ monolayer, the total DOS shown in Figure 6a demonstrates a pattern for a semiconductor with an energy gap about 0.81 eV. The PDOS introduced by N and H atoms of gas molecules below E_F and above 0.81 eV is marked in blue and cyan lines as shown in Figure 6a. There is no obviously change of the electronic structure of the pristine SnSe₂ as shown in Figure 2a, which is consistent with our previous work [8].

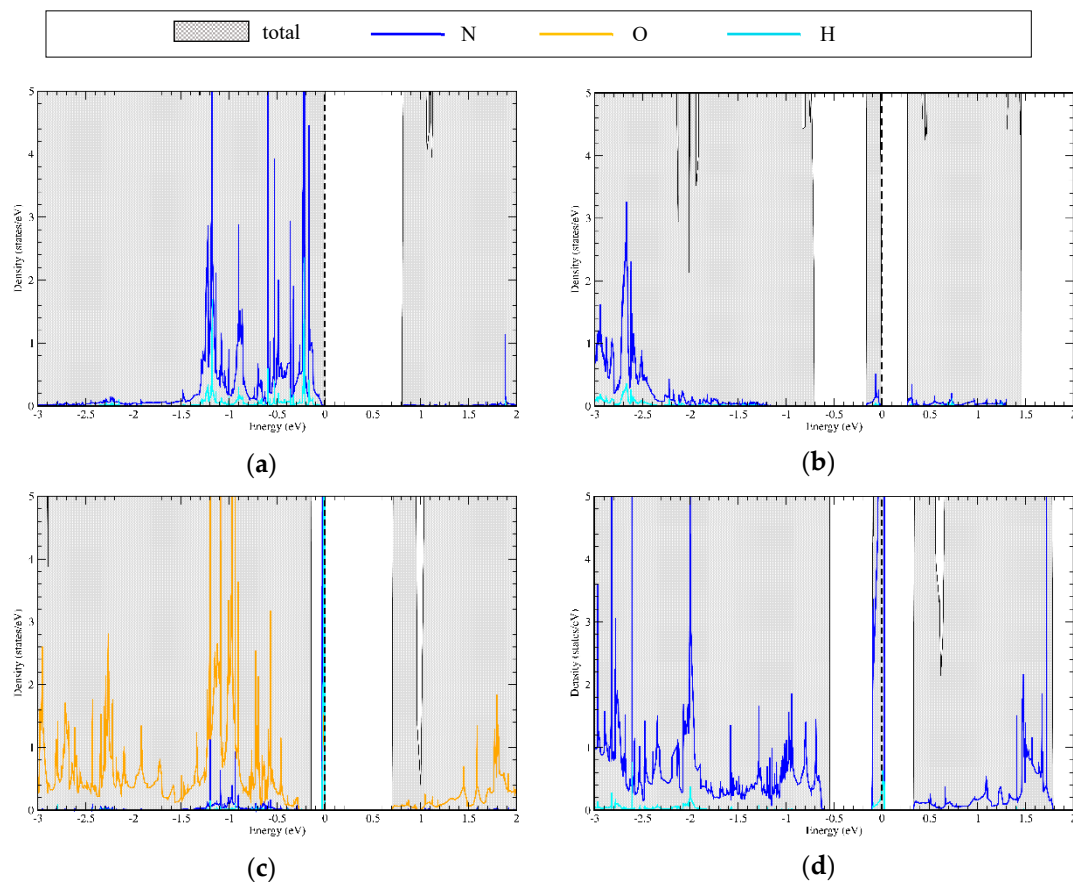


Figure 6. DOS of NH_3 adsorption on the (a)pristine, (b)Se vacancy, (c)O-doped and (d)N-doped SnSe_2 monolayer. The shadowed area is the total DOS. The blue, orange, cyan lines are the PDOS of N, O, H, respectively. The E_F is denoted by a dashed line and shift to zero.

When NH_3 adsorbed on the Se-vacancy SnSe_2 monolayer, the total DOS presents a bandwidth in energy range of -0.17 eV to E_F as shown in Figure 6b. The DOS pattern of Figure 6b is a semiconductor with energy gap about 0.27 eV. Only a small amount of PDOS contributed by N and H atoms of gas molecule is located the aforementioned bandwidth. This is so that NH_3 adsorption does not induce obvious difference on the DOS of the Se-vacancy SnSe_2 without adsorption as shown in Figure 2b.

For the O-doped SnSe_2 monolayer with NH_3 adsorption, the total DOS presents a flat band below E_F as shown in Figure 6c. A large amount of PDOS contributed by N and H atoms of gas molecules is located in the aforementioned flat band denoted by blue and cyan lines in Figure 6c. Because the flat band is located below E_F , the DOS pattern of Figure 6c is a semiconductor with energy gap about 0.70 eV. Therefore, the NH_3 adsorption does not change the pattern of DOS of the O-doped SnSe_2 monolayer as shown in Figure 2c.

For the N-doped SnSe_2 monolayer with NH_3 adsorption, the total DOS presents a trap state across E_F in the energy range about -0.10 eV to -0.03 eV as shown in Figure 6d. A large amount of PDOS induced by N and H atoms of gas molecules is located in the aforementioned trap state. The trap state responds to a flat band which would decrease the mobility of the SnSe_2 systems after gas adsorption. The pattern of DOS in Figure 6d is different from that of the N-doped SnSe_2 monolayer without adsorption as shown in Figure 2d.

Comparing the DOS of NH_3 adsorption on different SnSe_2 monolayers as shown in Figure 6a–d with the SnSe_2 monolayers without adsorption as shown in Figure 2a–d, only the N-doped SnSe_2 monolayer could induce obvious differences of electronic structure before/after NH_3 adsorption.

4. Discussion

We discuss the gas-sensing parameters, including E_{ad} and ΔQ_b , compared to gas molecules adsorbed on the pristine SnSe₂ monolayer and have demonstrated the high selectivity and sensitivity of the defective and doped SnSe₂ monolayer for gas-sensor candidates. The alteration of electronic structure is reflected by the change in electrical conductance of the SnSe₂ monolayers. We also discuss the DOS of gas adsorptions in the SnSe₂ monolayers to illustrate the change in the electrical conductance due to alteration of the electronic structure.

4.1. Gas Molecules on the Se-Vacancy SnSe₂ Monolayer

When NO₂ adsorbed on the Se-vacancy SnSe₂ monolayer, the values of $E_{ad} = -1.84$ eV and $\Delta Q_b = -0.926e$ were the maximum among that of the SnSe₂ monolayers. This reveals strong interaction between NO₂ molecule and the Se-vacancy SnSe₂ monolayer. For the Se-vacancy SnSe₂ monolayer, NO₂ adsorption induces wide-ranging trap states crossover E_F to decrease the carrier mobility as represented by the pattern of DOS in Figure 4b.

However, the NH₃ molecule is adsorbed on the Se-vacancy SnSe₂ monolayer with higher $E_{ad} = -0.82$ eV and lower $\Delta Q_b = 0.016e$ compared to the pristine SnSe₂ monolayer ($E_{ad} = -0.18$ eV, $\Delta Q_b = 0.028e$ [8]). NH₃ adsorption on the Se-vacancy SnSe₂ monolayer contributes DOS below E_F , as shown in Figure 6b. However, the charge transfer amount of NH₃ on the Se-vacancy SnSe₂ monolayer is smaller than that of NH₃ on the pristine SnSe₂ monolayer. Therefore, we cannot be sure of the conductivity difference of the Se-vacancy SnSe₂ monolayer with/without NH₃ adsorption.

The Se-vacancy SnSe₂ monolayer shows excellent sensitivity for NO₂ molecules, whereas the Se-vacancy SnSe₂ monolayer cannot show obvious conductivity difference for NH₃ adsorption. In brief, the Se-vacancy SnSe₂ monolayer shows enhancement only for NO₂.

4.2. Gas Molecules on the O-Doped SnSe₂ Monolayer

When NO₂ adsorbed on the O-doped SnSe₂ monolayer, the values of $E_{ad} = -0.32$ eV and $\Delta Q_b = -0.145e$ are close to the molecule on the pristine SnSe₂ monolayer ($E_{ad} = -0.29$ eV, $\Delta Q_b = -0.164e$ [8]). The DOS of the O-doped SnSe₂ monolayer is similar to that of the pristine SnSe₂ monolayer, so that the similar appearance of DOS occurs in NO₂ adsorption on the pristine and O-doped SnSe₂ monolayer as shown in Figure 4a,c. The DOS of NO₂ on the O-doped SnSe₂ monolayer induces trap state crossover E_F and decreases the carrier mobility. The electronic structure altered by NO₂ adsorbed on the O-doped SnSe₂ monolayer would contribute a change of electrical conductance, just like NO₂ adsorption on the pristine SnSe₂ monolayer [8].

On the other hand, the value of $E_{ad} = -0.13$ eV and $\Delta Q_b = 0.000e$ for NH₃ on the O-doped SnSe₂ monolayer are both the minimum among the NH₃ adsorption. The DOS of NH₃ on the O-doped SnSe₂ monolayer is below the E_F , which results in similar electrical properties with the O-doped SnSe₂ monolayer without gas adsorption. This means that there is no obvious change of electrical conductance.

In conclusion, gas molecules on the O-doped SnSe₂ monolayer shows high sensitivity for NO₂ adsorption and even with a weaker detection for NH₃, compared to gases on the pristine SnSe₂. This result indicates that the O-doped SnSe₂ monolayer has better selectivity to these two gases in comparison with pristine SnSe₂.

4.3. Gas Molecules on the N-Doped SnSe₂ Monolayer

When NO₂ adsorbed on the N-doped SnSe₂ monolayer, $E_{ad} = -2.98$ eV is the maximum among the NO₂ adsorption and $\Delta Q_b = -0.368e$ has relatively high value. It indicates that the strong interaction occurred between NO₂ molecule and the N-doped SnSe₂ monolayer. Moreover, the DOS of the N-doped SnSe₂ monolayer before/after NO₂ adsorption are totally different, as shown in Figures 2d and 4d.

Compared to the DOS of the N-doped SnSe₂ monolayer before/after NO₂ adsorption, the DOS crossover E_F of the N-doped SnSe₂ moves to below the E_F.

When NH₃ is adsorbed on the N-doped SnSe₂ monolayer, E_{ad} = −0.36 eV also has a greater value than that on the pristine SnSe₂ monolayer and ΔQ_b = 0.215e has a maximum value. In the DOS of NH₃ adsorbed on the N-doped SnSe₂ monolayer, the trap state is induced to decrease the carrier mobility. This implies that there would be an obvious change of electrical conductance. The N-doped atom is high sensitivity gas sensor for NO₂ and NH₃ shown as in our DFT calculation.

When setting gas molecules on the N-doped SnSe₂, it reveals obvious enhancement for both NO₂ and NH₃ adsorption.

5. Conclusions

In summary, the adsorption of NO₂ and NH₃ on the Se-vacancy, O-doped and N-doped SnSe₂ monolayer are investigated and compared to the pristine SnSe₂ monolayer. Due to the high adsorption energy and large charge transfer of gas adsorption on the Se-vacancy SnSe₂ monolayer, the Se-vacancy SnSe₂ monolayer shows a better sensitivity only to NO₂. However, the sensitivity of NH₃ adsorbed on the Se-vacancy SnSe₂ monolayer has higher adsorption energy but lower charge transfer amount than the pristine SnSe₂ monolayer. Furthermore, the O-doped SnSe₂ monolayer has similar interaction with NO₂ with the pristine SnSe₂ monolayer, but weaker interaction with NH₃ than the pristine SnSe₂ monolayer. This indicates that the O-doped SnSe₂ monolayer has similar sensitivity to the pristine SnSe₂ monolayer and better selectivity than the pristine SnSe₂ monolayer. The N-doped SnSe₂ strongly interacts both with NO₂ and NH₃ and shows obvious sensing enhancement for those two gases. In brief, the vacancy and doped SnSe₂ monolayers can enhance the selectivity and sensitivity of gas sensing for NO₂ and NH₃ molecules. This work demonstrates the potential of the SnSe₂-based gas sensors by introducing defects and dopants in the SnSe₂ monolayer.

Supplementary Materials: The following are available online at <http://www.mdpi.com/2076-3417/10/5/1623/s1>: Figure S1: The initial configurations of the defective SnSe₂ monolayers adsorbing NO₂ molecule with N-top and N-bottom orientations, Figure S2: The initial configurations of the defective SnSe₂ monolayers adsorbing NH₃ molecule with N-top and N-bottom orientations.

Author Contributions: W.-Y.C.: Data curation, Data analysis, writing – original draft & review & editing; H.-R.F.: Conceptualization, writing – review & editing; C.-R.C.: Supervision, Writing – review & editing. All authors have read and agreed to the published version of the manuscript.

Funding: This research was funded by Ministry of Science and Technology of R. O. C. under grant No. MOST 107-2112-M-002-013-MY3.

Acknowledgments: C. R. Chang thanks for supports from Ministry of Science and Technology of R. O. C. under grant No. MOST 107-2112-M-002-013-MY3. H.R. Fuh thanks for supports from Ministry of Science and Technology of R. O. C. under grant No. MOST 107-2112-M-155-001-MY3. W. Y. Cheng and H. R. Fuh thanks the computer and information networking center in National Taiwan University, Taiwan for the computational support.

Conflicts of Interest: The authors declare no conflict of interest.

References

1. Liu, X.; Ma, T.; Pinna, N.; Zhang, J. Two-dimensional nanostructured materials for gas sensing. *Adv. Funct. Mater.* **2017**, *27*, 1702168. [[CrossRef](#)]
2. Kim, Y.H.; Kim, K.Y.; Choi, Y.R.; Shim, Y.S.; Jeon, J.M.; Lee, J.H.; Kim, S.Y.; Han, S.; Jang, H.W. Ultrasensitive reversible oxygen sensing by using liquid-exfoliated MoS₂ nanoparticles. *J. Mater. Chem. A* **2016**, *4*, 6070–6076. [[CrossRef](#)]
3. Ou, J.Z.; Ge, W.Y.; Carey, B.; Daeneke, T.; Rotbart, A.; Shan, W.; Wang, Y.C.; Fu, Z.Q.; Chrimes, A.F.; Wiodarski, W.; et al. Physisorption-based charge transfer in two-dimensional SnS₂ for selective and reversible NO₂ gas sensing. *ACS Nano*. **2015**, *9*, 10313–10323. [[CrossRef](#)] [[PubMed](#)]
4. Yu, P.; Yu, X.C.; Lu, W.L.; Lin, H.; Sun, L.F.; Du, K.Z.; Liu, F.C.; Fu, W.; Zeng, Q.S.; Shen, Z.X.; et al. Fast photoresponse from 1T tin diselenide atomic layers. *Adv. Funct. Mater.* **2016**, *26*, 137. [[CrossRef](#)]

5. Wu, Y.X.; Li, W.; Faghaninia, A.; Chen, Z.W.; Li, J.; Zhang, X.Y.; Gao, B.; Lin, S.Q.; Zhou, B.Q.; Jain, A.; et al. Promising thermoelectric performance in van der Waals layered SnSe₂. *Mater. Today Phys.* **2017**, *3*, 127–136. [[CrossRef](#)]
6. Yang, Z.; Su, C.; Wang, S.; Han, Y.; Chen, X.; Xu, S.; Zhou, Z.; Hu, N.; Su, Y.; Zeng, M. Highly sensitive NO₂ gas sensors based on hexagonal SnS₂ nanoplates operating at room temperature. *Nanotechnology* **2019**, *31*, 075501. [[CrossRef](#)]
7. Yan, W.J.; Chen, D.Y.; Fuh, H.R.; Li, Y.L.; Zhang, D.; Liu, H.J.; Wu, G.; Zhang, L.; Ren, X.K.; Cho, J.; et al. Photo-enhanced gas sensing of SnS₂ with nanoscale defects. *RSC Adv.* **2019**, *9*, 626–635. [[CrossRef](#)]
8. Moreira, O.L.C.; Cheng, W.Y.; Fuh, H.R.; Chien, W.C.; Yang, W.J.; Fei, H.F.; Xu, H.J.; Zhang, D.; Chen, Y.H.; Zhao, Y.F.; et al. High selectivity gas sensing and charge transfer of SnSe₂. *ACS Sens.* **2019**, *4*, 2546–2552. [[CrossRef](#)]
9. Huang, Y.C.; Zhou, D.; Chen, X.; Liu, H.; Wang, C.; Wang, S. First-principles study on doping of SnSe₂ monolayers. *Chem. Phys. Chem.* **2016**, *17*, 375–379. [[CrossRef](#)]
10. Hyeon, D.S.; Oh, M.S.; Kim, J.T.; Lee, Y.J.; Kim, S.I.; Moon, S.P.; Hamayoun, N.; Kim, S.W.; Lee, K.H.; Bang, J.; et al. Electrical properties of bromine doped SnSe₂ van der Waals material. *J. Phys. D Appl. Phys.* **2018**, *51*, 455102. [[CrossRef](#)]
11. Kim, S.I.; Hwang, S.; Kim, S.Y.; Lee, W.J.; Jung, D.W.; Moon, K.S.; Park, H.J.; Cho, Y.J.; Cho, Y.H.; Kim, J.H.; et al. Metallic conduction induced by direct anion site doping in layered SnSe. *Sci. Rep.* **2016**, *6*, 19733. [[CrossRef](#)] [[PubMed](#)]
12. Kim, J.T.; Hyeon, D.S.; Hanzawa, K.; Kanai, A.; Kim, S.Y.; Lee, Y.J.; Hosono, H.; Bang, J.; Lee, K. Role of fluorine in two-dimensional dichalcogenide of SnSe₂. *Sci. Rep.* **2018**, *8*, 1645. [[CrossRef](#)] [[PubMed](#)]
13. Xiang, H.; Xu, B.; Xia, Y.D.; Yin, J.; Liu, Z.G. Strain tunable magnetism in SnX₂ (X = S, Se) monolayers by hole doping. *Sci. Rep.* **2016**, *6*, 39218. [[CrossRef](#)] [[PubMed](#)]
14. Zhang, Y.H.; Chen, Y.B.; Zhou, K.G.; Liu, C.H.; Zeng, J.; Zhang, H.L.; Peng, Y. Improving gas sensing properties of graphene by introducing dopants and defects: A first-principles study. *Nanotechnology* **2009**, *20*, 185504. [[CrossRef](#)]
15. Lee, G.; Yang, G.; Cho, A.; Han, J.W.; Kim, J. Defect-engineered graphene chemical sensors with ultrahigh sensitivity. *Phys. Chem. Chem. Phys.* **2016**, *18*, 14198–14204. [[CrossRef](#)]
16. Alalamy, F.A.S.; Balchin, A.A.; White, M. Expansivities and thermal-degradation of some layer compounds. *J. Mater. Sci.* **1977**, *12*, 2037–2042. [[CrossRef](#)]
17. Momma, K.; Izumi, F. VESTA3 for three-dimensional visualization of crystal, volumetric and morphology data. *J. Appl. Crystallogr.* **2011**, *44*, 1272–1276. [[CrossRef](#)]
18. Perdew, J.P.; Burke, K.; Ernzerhof, M. Generalized gradient approximation made simple. *Phys. Rev. Lett.* **1996**, *77*, 3865–3868. [[CrossRef](#)]
19. Kresse, G.; Joubert, D. From ultrasoft pseudopotentials to the projector augmented-wave method. *Phys. Rev. B* **1999**, *59*, 1758–1775. [[CrossRef](#)]
20. Zou, D.F.; Yu, C.B.; Li, Y.H.; Ou, Y.; Gao, Y.Y. Pressure-induced enhancement in the thermoelectric properties of monolayer and bilayer SnSe. *R. Soc. Open Sci.* **2018**, *5*, 14. [[CrossRef](#)]
21. Henkelman, G.; Arnaldsson, A.; Jonsson, H. A fast and robust algorithm for Bader decomposition of charge density. *Comput. Mater. Sci.* **2006**, *36*, 354–360. [[CrossRef](#)]

